Supporting Online Material for

Structural Asymmetry of AcrB Trimer Suggests a Peristaltic Pump Mechanism

Markus A. Seeger, André Schiefner, Thomas Eicher,
François Verrey, Kay Diederichs, Klaas M. Pos*

*To whom correspondence should be addressed. E-mail: kmpos@access.unizh.ch

Published 1 September 2006, *Science* **313**, 1295 (2006)
DOI: 10.1126/science.1131542

This PDF file includes:

Supporting Online Material

Structural Asymmetry of AcrB Trimer suggests a Peristaltic Pump Mechanism

Markus A. Seeger, André Schiefner, Thomas Eicher, François Verrey, Kay Diederichs & Klaas M. Pos

Materials and Methods

Materials and Methods

Crystallization

Purification of AcrB was carried out as described previously (S*1*) with slight modifications. Solubilization was carried out with 2 % n-dodecyl-β-maltoside instead of 2 % cyclohexyl-n-hexyl-β-D-maltoside and AcrB was purified using buffers containing 200 mM NaCl instead of 100 mM NaCl. Finally the protein was washed and concentrated in 10 mM potassium-phosphate, pH 7.0, and 0.05 % cyclohexyl-n-hexyl-β-D-maltoside. Prior to crystallization, the protein concentration was adjusted to 8 - 12 mg ml^{-1}, ethidium or dequalinium was added (400 µM or 200 µM final concentration, respectively) and the sample was passed through a 0.22 µm Milex-GV filter unit (Millipore). Crystals were grown by hanging-drop vapor diffusion at 17 °C by mixing equal volumes of protein (8 - 12 mg ml^{-1}) and reservoir solution. AcrB crystals of space group *C*2 and *P*1 were grown over a reservoir solution of 5 % polyethylene glycol 400, 16-22 % polyethylene glycol 300, 8-11 % glycerol and 70 mM Na^+-citrate pH 4.6. Crystals appeared within 3 - 4 days (*C*2) or 10 - 20 days (*P*1) and reached a maximal size of 0.8 x 0.5 x 0.2 mm^3 (*C*2) or 0.3 x 0.2 x 0.15 mm^3 (*P*1), respectively. Addition of drugs (ethidium or dequalinium) was beneficial to obtain high quality crystals. These were gently removed from the drop and without further cryoprotection flash frozen in liquid propane prior to data collection.

X-ray diffraction dataset analysis and refinement procedure

Datasets from *R*32 and *C*2 crystals were collected at the beamline X06SA of the Swiss Light Source (Paul Scherrer Institut, Villigen, Switzerland) (wavelength λ: 0.9774 and 1.0 Å, respectively). Datasets from the *P*1 crystal were collected at beamline ID29 of the ESRF (Grenoble, France)(wavelength λ: 0.9737 Å). Data reduction was done with the XDS package (S*2*). The structures were solved by molecular replacement using MOLREP (S*3*) or PHASER (S*4*). As search models 1IWG (S*5*) and a modified version of 1iwg (model2 (S*6*)) were used. Refinement in *C*2 and *P*1 was performed with the program REFMAC5 (S*7*) starting with 20 cycles of rigid body refinement followed by restrained refinement with TLS restraints (S*8*). The program SHELXL (S*9*) was used for refinement in the trigonal space groups, to be able to apply the appropriate computational treatment of twinning, and to consistently compare results obtained

with and without provision for twinning. Due to the large structural deviations observed between the monomers (Table S2), non-crystallographic symmetry restraints were not employed during refinement. Model rebuilding was performed using the program COOT (S*10*). Tunnels and cavities were calculated using MAMA (S*11*), VOIDOO (S*12*) and visualised with CAVER (S*13*). Figures were made using PyMOL (http://pymol.sourceforge.net/). Secondary structures were assigned with DSSP (S*14*).

Our analysis revealed that those crystals that appeared to be *R*32 were in fact twinned *R*3 crystals. In these crystals, the two-fold non-crystallographic axis coincides with the twinning axis, resulting in a pseudo-R32 diffraction pattern; a situation that is often encountered in R3. Due to the presence of non-crystallographic symmetry, detection of the existence of twinning was not possible by inspection of intensity statistics (S*15*); rather we found that restrained refinement in SHELXL (S*9*) resulted in significantly reduced R and R_{free} when a single parameter, the twinning fraction α, was optimized in the refinement. In many of our datasets, this parameter refined towards 0.5 (thus indicating perfect twinning); in some datasets, we observe lower twinning fractions (between 0.3 and 0.45). The Ramachandran statistics for the refined structures were determined using PROCHECK (S*16*) and were as follows (core, allowed, generously allowed and disallowed in %): AcrB-*C*2: 90.0, 9.5, 0.4, 0.1; AcrB-*P*1: 90.4, 9.2, 0.3, 0.1; AcrB-*R* (*R*32): 80.2, 18.5, 1.0, 0.2; AcrB-*R* (*R*3, not accounting for twinning): 79.6, 18.4, 1.8, 0.2: AcrB-*R*-twin (*R*3, accounting for twinning): 90.6, 18.1, 1.1, 0.2.

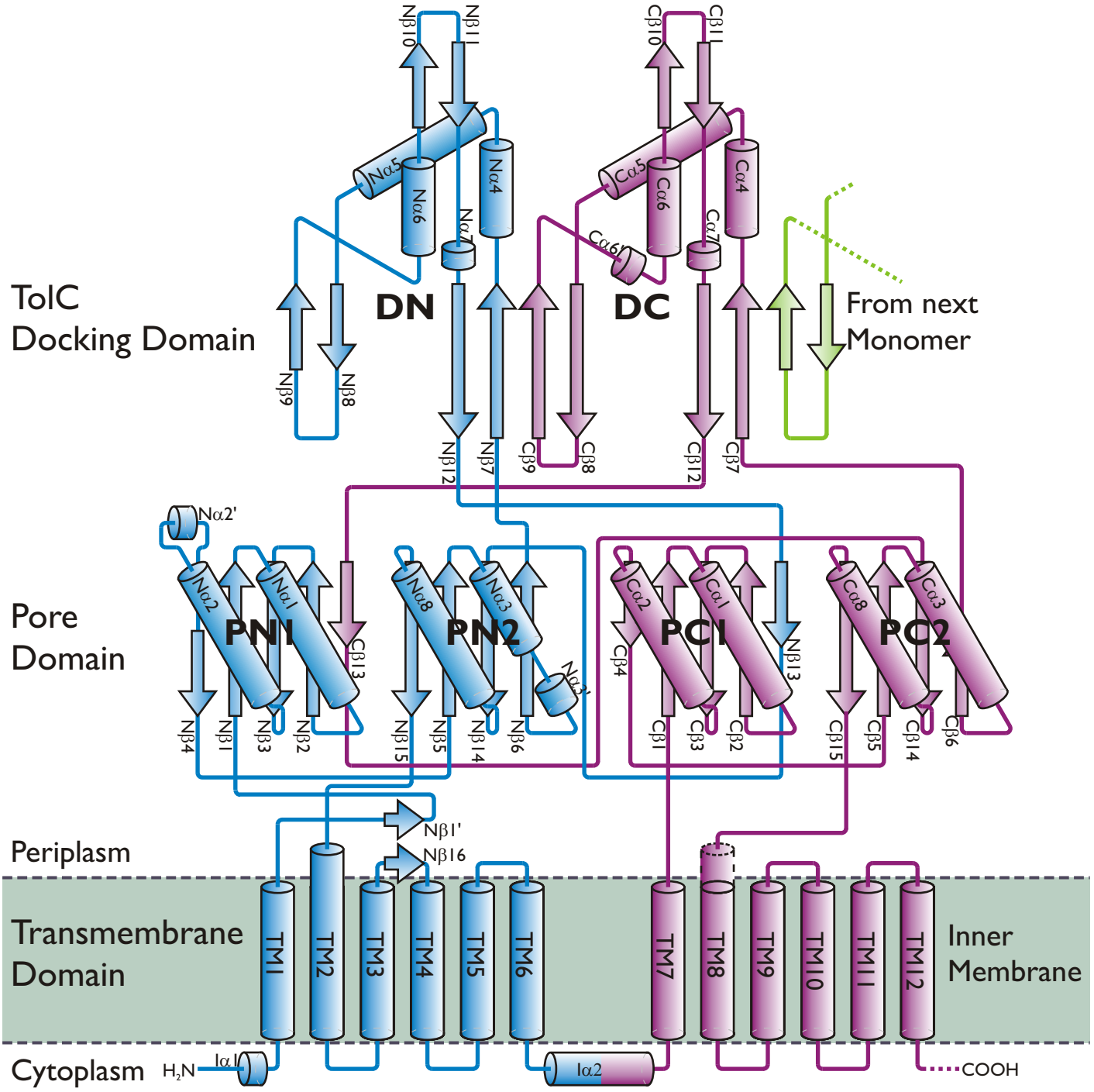

Fig. S1. AcrB monomer secondary structure scheme (residues 2-1033). For this representation the designations and the representation style were adapted from Murakami et al. (*S5*) and extended according to the new asymmetric structure data. The pore domain contains four subdomains, PN1, PN2, PC1 and PC2. The TolC-docking domain has two subdomains, DN and DC. TM, transmembrane helices; Nα, Nβ, Cα and Cβ are α-helices and β-sheets of the N-terminal part or the C-terminal part of the periplasmic domain. Iα2 is the cross-α-helix at the cytoplasmic side. N- and C-terminal halves are depicted in blue and magenta, respectively. The intermonomer connecting loop from the adjacent monomer (hairpin structure protruding from one monomer into the next) is depicted in green.

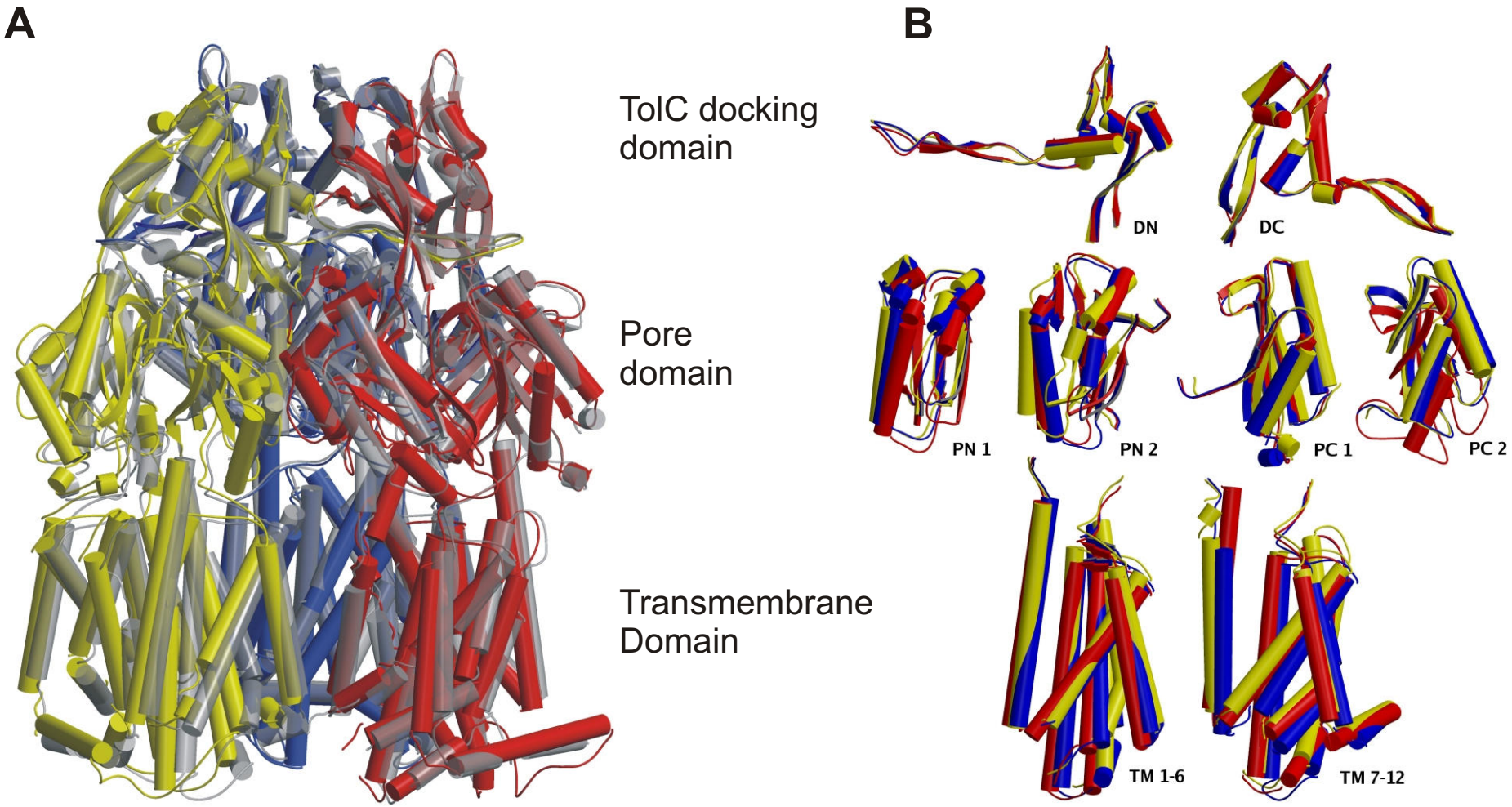

Fig. S2. Main structural differences of the AcrB monomers. α-helices are depicted as cylinders, β-sheets as flat arrows and loops as lines. The structures in blue, yellow and red represent the L, T and O monomers, respectively. (**A**) Side view of the asymmetric AcrB superimposed onto the symmetric AcrB trimer model depicted in transparent grey. (**B**) Superimposition of the AcrB subdomain structures. The largest conformational changes are observed in the PN1 (red, O), PN2 (yellow, T) and PC2 (red, O) subdomains. The monomers were superimposed using the program SUPERPOSE matching the DN (residues 181-272) and DC (residues 724-812) subdomains.

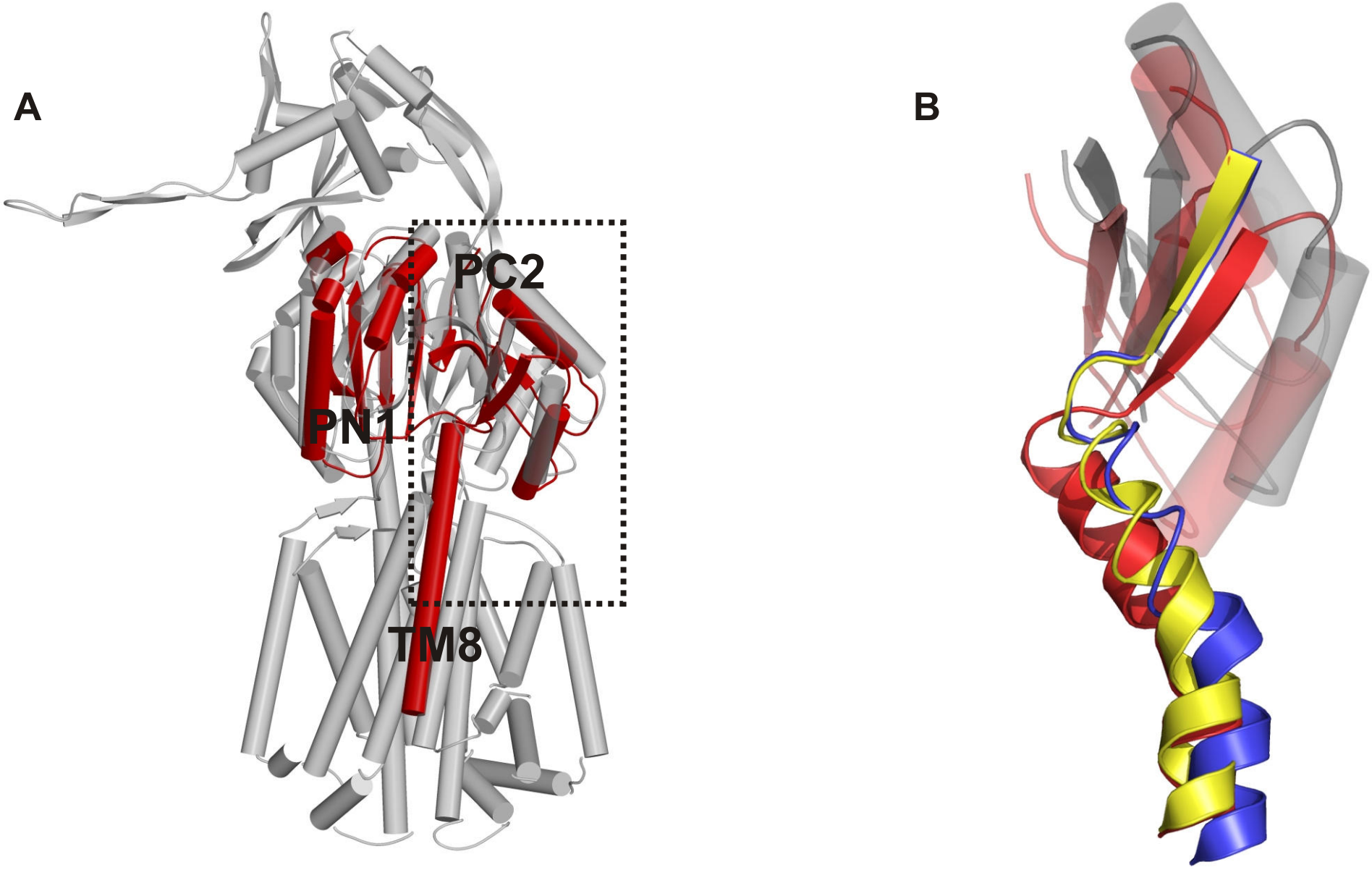

Fig. S3. (A) Side view superimposition of the AcrB L monomer (grey) and the PN1, PC2 subdomains as well as TM8 of the O monomer (red). **(B)** In a close-up view of the boxed region of (A) the N-terminal part of TM8 (residues 859 to 880) and the PC2 subdomain (residues 679-721 and 822-858) are superimposed. The structures in blue, yellow and red represent the conformations of the TM8 and the C-terminal β-sheets (Cβ15) of the PC2 subdomains of the L, T and O monomers, respectively. The rest of the PC2 subdomain is depicted in transparent grey (L and T monomers) or red (O monomer).

Table S1: Crystallographic data and refinement

	AcrB-*C*2	AcrB-*P*1	AcrB-*R*	AcrB-*R*	AcrB-*R*-twin
Data collection					
Space group*	*C*2	*P*1	*R*32	*R*3	*R*3
Cell dimensions					
a (Å)	222.8	127.3	143.7	143.7	143.7
b (Å)	134.1	134.9	143.7	143.7	143.7
c (Å)	161.0	140.8	513.6	513.6	513.6
α (°)	90	103.9	90	90	90
β (°)	98.2	94.6	90	90	90
γ (°)	90	90.1	120	120	120
Resolution (Å)†	2.9 (3.07-2.9)	3.0 (3.1-3.0)	2.65 (2.75-2.65)	2.65 (2.75-2.65)	2.65 (2.75-2.65)
R_{meas} (S*17*)(%)	8.9 (112.1)	15.5 (89.1)	8.9 (64.0)	9.0 (67.9)	9.0 (67.9)
I/σ_I	13.43 (1.5)	8.4 (1.9)	16.2 (2.3)	11.7 (1.7)	11.7 (1.7)
Completeness (%)	98.6 (93.2)	98.8 (99.9)	99.2 (89.5)	98.8 (81.4)	98.8 (81.4)
Redundancy	4.2 (4.1)	4.0 (3.7)	9.1 (3.4)	4.7 (1.9)	4.7 (1.9)
Refinement					
Trimer model	asymmetric	asymmetric	symmetric	symmetric	symmetric
Program (S*7,* S*9*)	REFMAC	REFMAC	SHELXL	SHELXL	SHELXL
Twinning fraction				0.0	0.5
Resolution (Å)	29.5-2.9 (2.98-2.9)	29.8-3.0 (3.08-3.0)	10-2.65 (2.70-2.65)	10-2.65 (2.70-2.65)	10-2.65 (2.70-2.65)
No. reflections	98361 (7154)	172056 (12568)	55279 (5710)	105881 (10611)	105881 (10611)
R_{work}	22.6 (34.3)	23.1 (33.2)	29.4 (38.9)	29.5 (41.5)	25.9 (35.5)
R_{free}‡	26.7 (37.3)	27.6 (37.6)	38.2 (n.d.)	39.0 (n.d.)	35.6 (n.d.)
No. atoms					
Protein residues	3108§	6192‖	1030	2060	2060
B-factors					
Protein	74.0	51.4	90.9	87.7	81.7
R.m.s deviations					
Bond lengths (Å)	0.007	0.007	0.004	0.004	0.005
Bond angles (°)	1.1	1.1	1.1	1.1	1.3

*AcrB-*C*2, AcrB-*P*1, AcrB-*R* data are from measurements from one crystal each. The *R*3 and *R*32 data differ only in space group assignment. AcrB-*R*-twin denotes that SHELXL (S*9*) accounted for twinning during refinement.

†Highest resolution shell is shown in parenthesis.

‡ Five percent of the reflections were set aside for calculation of the R_{free} value.

§L and O monomer amino acids 2-1033 and *T* monomer amino acids 2-1045.

‖L, T and O monomer amino acids 2-1033.

Table S2 **Root-mean-square deviations (Å) of C_α coordinates between monomers* of the *C*2, *P*1 and *R*32 crystal forms, for the common residue range 2-1031**

Crystal form		*C*2			*P*1						*R*32
	Monomer	L	T	O	L	T	O	L’	T’	O’	
	L	-	2.11	3.09	0.32	2.02	3.06	0.30	2.10	3.04	0.90
*C*2	T	-	-	3.10	2.06	0.42	3.13	2.12	0.36	3.11	1.82
	O	-	-	-	3.07	3.12	0.32	3.16	3.18	0.31	3.00
	L	-	-	-	-	1.97	3.04	0.27	2.05	3.02	0.88
	T	-	-	-	-	-	3.14	2.02	0.28	3.12	1.78
*P*1	O	-	-	-	-	-	-	3.12	3.20	0.25	2.98
	L’	-	-	-	-	-	-	-	2.10	3.10	0.95
	T’	-	-	-	-	-	-	-	-	3.18	1.82
	O’	-	-	-	-	-	-	-	-	-	2.97

*The L, T and O monomers map to the A, B and C chains of the *P*1 and *C*2 structure model. L’, T’ and O’ correspond to the D, E and F chains of the *P*1 structure model.

References

S1. K. M. Pos, K. Diederichs, *Acta Crystallogr. Biol. Crystallogr.* **D58**, 1865 (2002).
S2. W. Kabsch, *J. Appl. Cryst.*, 795 (1993).
S3. A. A. Vagin, Teplyakov, A, *J Appl. Cryst.*, 1022 (1997).
S4. L. C. Storoni, A. J. McCoy, R. J. Read, *Acta Crystallogr. Biol. Crystallogr.* **D60**, 432 (2004).
S5. S. Murakami, R. Nakashima, E. Yamashita, A. Yamaguchi, *Nature* **419**, 587 (2002).
S6. K. M. Pos, A. Schiefner, M. A. Seeger, K. Diederichs, *FEBS Lett.* **564**, 333 (2004).
S7. G. N. Murshudov, Vagin, A. A., Dodson, E. J., *Acta Crystallogr. Biol. Crystallogr.* **D53**, 240 (1997).
S8. M. D. Winn, M. N. Isupov, G. N. Murshudov, *Acta Crystallogr. Biol. Crystallogr.* **D57**, 122 (2001).
S9. G. M. Sheldrick, T. R. Schneider, *Methods Enzymol.* **277** 319 (1997).
S10. P. Emsley, K. Cowtan, *Acta Crystallogr. Biol. Crystallogr.* **D60**, 2126 (2004).
S11. G. J. Kleywegt, T. A. Jones, *Acta Crystallogr. Biol. Crystallogr.* **D55**, 941 (1999).
S12. G. J. Kleywegt, T. A. Jones, *Acta Crystallogr. Biol. Crystallogr.* **D50**, 178 (1994).
S13. O. M. Petrek M., Banas P., Koca J., Damborsky J., (2006).
S14. W. Kabsch, C. Sander, *Biopolymers* **22**, 2577 (1983).
S15. A. A. Lebedev, A. A. Vagin, G. N. Murshudov, *Acta Crystallogr. Biol. Crystallogr.* **D62**, 83 (2006).
S16. R. A. Laskowski, M. W. MacArthur, D. S. Moss, J. M. Thornton, *J. Appl. Crystallogr.* **26**, 283–291 (1993).
S17. K. Diederichs, P. A. Karplus, *Nat. Struct. Biol.* **4**, 269 (1997).